ORGAN APPROXIMATION IN μCT DATA WITH LOW SOFT TISSUE CONTRAST USING AN ARTICULATED WHOLE-BODY ATLAS

M. Baiker[1], J. Dijkstra[1], I. Que[2], C. W. G. M. Löwik[2], J. H. C. Reiber[1] and B. P. F. Lelieveldt[1]

[1]Division of Image Processing
Department of Radiology, Leiden University
Medical Center, The Netherlands

[2]Department of Endocrinology
Leiden University Medical Center
The Netherlands

ABSTRACT

In this article, we present an approach for organ approximation in low contrast μCT data of mice using a whole-body mouse atlas (Segars et al. [1]). Starting from a set of landmarks on bone and joint locations, further correspondences are derived on surface representations of the lung by atlas-based registration and on the skin by employing a local geodesic shape context. Subsequently, landmarks on the skeleton, the lung and the skin are used to constrain a Thin-Plate-Spline (TPS) based mapping of major organs from the atlas to the subject domain.
The feasibility of the method has been tested by means of 26 CT mouse datasets and a different whole-body mouse atlas (Digimouse [2]). Proper mapping of the lung and the skin as well as major organs could be achieved in all cases yielding a mean Euclidean distance between surface nodes of 0.42 ± 0.068 mm for the lung and 0.34 ± 0.036 mm for the skin. The performance of the organ interpolation has been assessed on basis of manual segmentations of two CT datasets of mice with injected contrast agent and the Digimouse. The calculated dice indices of volume overlap show significant improvement compared to earlier studies.

Index Terms— Geodesic shape context, μCT, TPS approximation, whole-body segmentation

1. INTRODUCTION

The availability of small animal whole-body imaging modalities (μCT and μMRI) adds a new dimension to animal experiments. It enables monitoring dynamic processes *in-vivo*, within a population and at subsequent time points, i.e. cross-sectional and longitudinal studies.
To be able to quantify disease and developmental processes in whole-body scans, it is necessary to capture and match the body as a whole. Also, in applications such as Bioluminescence Tomography, whole-body tissue models are required to improve the accuracy of light source reconstruction algorithms [3]. However, an animal body is a very complex system because it contains stiff (rigid) structures like bones next to elastic (non-rigid) structures like organs. This is further complicated by the fact that the body contains many articulated parts. As a result, the shape and the posture can vary significantly among animals and among acquisition time points.
Two strategies for matching objects with heterogeneous stiffness properties can be found in the literature: data-driven and model-driven approaches. Whole-body registration methods so far are all data-driven and therefore cannot handle large differences in posture and shape (Chaudhari et al.[4], Li et al. [5], Kovacevic et al. [6]). On the other hand, the model-driven approaches have been applied to subparts of a body only (Martin-Fernandez et al. [7], Papademetris et al. [8], Du Bois d'Aische et al. [9]). In addition, most methods need a significant amount of user interaction e.g. to define joint locations or segment bones prior to registration.
To be able to capture arbitrary shape and posture variations among subjects, we earlier presented a method to automatically register the entire skeleton of a subject by means of an articulated atlas [10]. Determination of whole-body posture and shape is based on the skeleton because it is the main determinant of whole-body posture. Furthermore at many locations of the animal body, as in the vicinity of the spine and the ribcage, organ location and extent are closely related to the skeleton.
Due to the high radiodensity of bone, μCT allows robust automated extraction of the skeleton from the data. However, most soft tissue areas in the animal body show only little contrast. As a result, intensity feature-based registration between an atlas and the subject is not possible for most soft tissues. However the atlas contains all major organs, which can therefore be mapped from the atlas to the subject domain. To this end, TPS [11] interpolation can be used, because this has proven to be suitable for biological applications. The necessary set of corresponding landmarks can be derived mainly from the skeleton except for the ventral and lateral abdomen, due to the missing bone content. Thus further lateral landmarks are needed to preserve body shape.

The contributions of this work are as follows:

- We present a method to derive a dense point correspondence on the lung and the skin, starting from a set of sparse bone landmarks.

- Based on this correspondence, we present a landmark-constrained TPS mapping of major organs from the mouse atlas to the subject that yields an approximation of organ position and extent.

2. METHODOLOGY

Besides bone, also the lung and the skin show sufficient contrast to enable robust segmentation from CT data. The registered skeleton allows initializing subsequent lung registration. Furthermore a sparse set of corresponding skin landmarks can be derived, since at many locations in the animal body, skin is very close to the skeleton. Based on this, a dense set of corresponding landmarks can be derived and together with the bone and lung landmarks be used to constrain a TPS based organ interpolation.

2.1. Determination of correspondences on the lung

The shape of the lung is strongly spatially constrained by the spine, the sternum and the ribs but still varies significantly between specimens. The choice of the registration strategy is a trade-off between speed and accuracy. Pilot experiments showed that rigid registration between atlas and subject lung allowing non-isotropic scaling to account for breathing does give satisfactory results. Correspondence is established using Iterative Closest Point matching (ICP [12]), based on the Euclidean distance between two surfaces as the error criterion.

2.2. Derivation of correspondences on the skin

Establishing correspondence between two skin surfaces in the most general case is very difficult. This is because dependent on how the animal is placed during acquisition, the shape can be almost rotation-symmetric to the longitudinal axis of the body, symmetric to the sagittal plane or symmetric to the transverse plane. Furthermore, the shape of an animal can differ significantly e.g. if two mice are positioned in prone and supine position respectively. The first issue can be resolved directly, if a registered skeleton is at hand. Then it is possible to determine a sparse set of corresponding landmarks on the surface of the animal skin by calculating the nodes with the smallest Euclidean distance from a set of bone landmarks. Having defined a sparse landmark set allows removing ambiguity during matching.

The second issue can be resolved by relying on a local shape context to identify corresponding nodes. The idea of matching shapes based on global shape contexts has been introduced by Belongie et al. [13]. However to be able to take local shape deformation into account, the representation has to be bending invariant. Using geodesic instead of Euclidean distances in a local context allows rendering the representation rotation, translation and bending invariant. While in general not scaling invariant, different animal sizes can be accounted for by normalization of the geodesic distances.

Let $P = \{p_1 \dots p_n\}$ and $Q = \{q_1 \dots q_m\}$ be the nodes of two surfaces to be matched and h_i and h_j be the histograms of geodesic distances from nodes p_i on P and q_j on Q to other nodes of the surface. The procedure of finding dense correspondence on the skin is as follows:

1. Initialize a list with corresponding skin nodes that are known (landmarks derived from skeleton registration)

Repeat for all elements in the correspondence list:

2. Select all nodes on P and Q in the vicinity (i.e. between a maximum and minimum geodesic distance and with a minimum distance to already known correspondences as shown in Figure 1, top) of the next element on the list
3. Calculate a local shape context based on geodesic distances towards K known corresponding nodes for the selected nodes in P and Q

Repeat steps 4-7 until no selected nodes are left:

4. Calculate the cost for matching two nodes p_i and q_j using the χ^2 test statistic [13]. $h_i(k)$ and $h_j(k)$ are histograms of geodesic distances:

$$C_{ij} = \frac{1}{2}\sum_{k=1}^{K}\frac{\left[h_i(k) - h_j(k)\right]^2}{h_i(k) + h_j(k)}$$

5. Find the best match as $\min(C_{ij})$
6. Add the found match to the list of correspondences
7. Remove the selected nodes whose geodesic distance to the newly found correspondence is too small

Due to the discretization of the surfaces, detected correspondences are generally not exact. To avoid the accumulation of small localization errors while progressing over the surface, determination of corresponding nodes should start at a coarse scale (in terms of inter-node distance) and, dependent on the amount of detail to be captured, continue at a smaller scale e.g. as proposed in Wang et al. [14].

2.3. TPS approximation of the organs

Based on landmarks on bone, lung and skin, organs can be warped from the atlas domain to the subject domain.

In its original form i.e. if used as an interpolant, the TPS does force landmarks in the source domain to fit landmarks in the target domain exactly. However in general small spatial errors may occur and this can cause local distortions of the mapping. A remedy is to allow small landmark localization errors and relax the constraint of interpolation towards approximation (thin-plate smoothing spline [15]).

3. EXPERIMENTAL RESULTS

To validate the method for determination of lung and skin correspondences, 3D data volumes were acquired of 26 mice *in-vivo* with a Skyscan 1178 µCT scanner (Kontich, Belgium). Animals were placed in prone and supine position with arbitrary limb position. The data was sub-sampled and smoothed yielding a voxel size of 320 x 320 x 320 μm^3 [10]. Surface representations of the skin and the lung have been generated automatically using labeled data volumes after thresholding and seeded region growing respectively. The lung surface has been registered using ICP and Levenberg-Marquardt minimization, initialized by landmarks on the spine and the sternum. The registration error (the mean Euclidean distance between surface nodes for 26 cases) decreased from 1.76 ± 0.49 mm to 0.42 ± 0.068 mm. For deriving correspondences on the skin surface we use a triangulated skin representation with 2000 nodes and a sparse set of 32 landmarks, derived from the joints, the spine and the skull. Geodesic distances were determined using the Fast Marching Algorithm [16] and the error criterion was based on the eight closest landmarks (i.e. K=8). The initial set was replenished by ≈120 landmarks from the skin all over the body and 30 landmarks on the lung, yielding a total set of ≈182 corresponding nodes (Figure 1, bottom) to constrain the TPS approximation. Note that for searching landmarks on the skin, the distal ends of the limbs have been excluded for this experiment since they do not contribute to the shape of organs. The mean Euclidean distance between atlas and subject skin nodes after the mapping including all 26 cases was 0.34 ± 0.036 mm. Results of two mice are shown in Figure 2.

To validate the organ approximation method, two mice with different contrast agents (Iomeron 400 [17], Fenestra LC [18]) have been scanned using µCT and the datasets were manually segmented (Amira V3.1, Mercury Computer Systems) by an expert. Quantitative assessment was performed by calculating dice indices of volume overlap for these two mice and the Digimouse atlas. The stomach, the spleen and the intestines have not been considered, due to the very large environmentally dependent variability of shape and location.

The manually segmented mice as well as the organ approximation used for derivation of dice indices are presented in Figure 3 and the results given in Table 1. Note that for the Digimouse we generated a virtual CT dataset based on the labeled volume to employ the same skin and lung extraction method as for the other datasets, because the labels are not registered to the raw CT data.

Registration of the lung, derivation of skin landmarks and organ approximation were implemented in Matlab 2007b and processing time was ≈2min on a standard desktop PC.

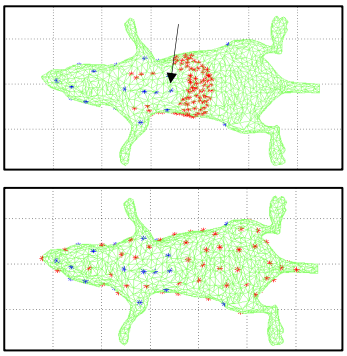

Figure 1: Possible new correspondences (red) based on a known landmark on the chest (arrow). Bottom: net of sparse (blue) and dense (red) correspondences

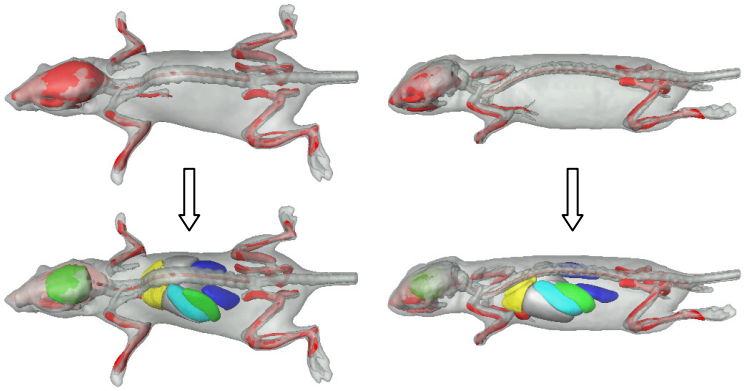

Figure 2: Organ approximation results. The subject skeleton is shown in grey and the atlas skeleton in red. The organs are brain (green), lung (yellow), heart (red), liver (grey), stomach (light blue), spleen (green) and kidneys (dark blue)

	Mouse in prone position			Mouse in supine position			Digimouse			Chaudhari et al. [4]
	Volume subject (mm^3)	Volume atlas	Dice index	Volume subject	Volume atlas	Dice index	Volume subject	Volume atlas	Dice index	Dice index
Skeleton	427.15	353.80	0.69	436.26	337.77	0.75	381.66	300.12	0.67	0.1572
Brain	325.03	421.20	0.76	352.67	433.11	0.81	359.47	386.81	0.88	0.7047
Heart	251.88	252.65	0.81	290.38	328.73	0.61	224.27	162.60	0.65	0.4673
Lung	465.41	519.68	0.70	721.89	696.00	0.82	383.26	314.96	0.75	0.4871
Liver	1332.81	1930.26	0.73	2140.86	2057.26	0.80	2007.07	1615.46	0.75	0.6508
Kidneys	354.83	210.17	0.48	392.76	265.71	0.60	495.10	300.82	0.60	0.4363

Table 1: Dice indices ($2*(V_s \cap V_a)/(V_s+V_a)$) for the skeleton (except spine and skull) and major organs

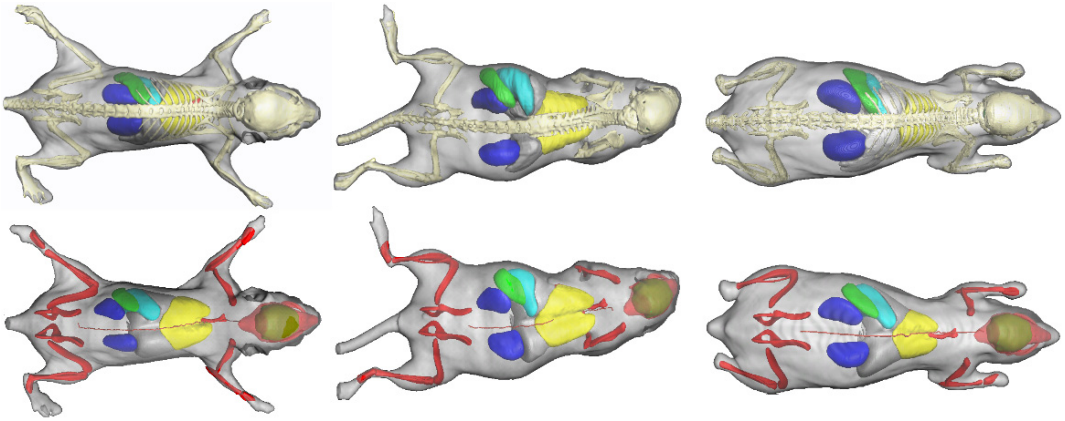

Figure 3: Manual segmentation (top row) versus automated skeleton registration and organ approximation (bottom row) for mice in prone (left column) and supine (middle column) position and for the Digimouse (hind paws are not included)

4. DISCUSSION AND CONCLUSION

While the skeleton registration has been validated elsewhere [10] we show here that the chosen registration for the lung and the subsequent derivation of landmarks on the skin leads to a close approximation of both with errors in the data resolution range, for all 26 cases. The calculated dice indices of volume overlap outperform previously documented results [4], especially for the skeleton. Above that, animals have been positioned during acquisition such that they significantly differed in posture and shape compared to each other and in particular compared to the used atlas and the Digimouse.

Detailed investigation of the dice indices leads to several observations. First, the difference in lung volume is relatively large for the Digimouse atlas. This is because using automated lung segmentation for the virtual CT dataset leads to an overestimation of the Digimouse lung. Since the heart approximation is greatly constrained by landmarks on the lung, its volume is underestimated for this dataset. Though the dice indices for the skeleton are high, its volume is systematically underestimated, since down-sampling and smoothing renders the joints as bone content. Therefore the joints contribute to the skeleton volume as well. Investigation of the approximated kidneys reveals occasional underestimation of their volume. The reason for this is the almost round cross section of the mouse atlas torso and the usually more elliptic cross-section of a subject torso. If the round torso has to be deformed to an ellipse, everything in between is squeezed, regardless if this is anatomically realistic or not.

In conclusion, the presented method is applicable for referencing of internal processes in molecular imaging research or whole-body segmentation (e.g. to provide a heterogeneous tissue model for bioluminescence tomography). Furthermore, the approximation result could also serve to initialize a subsequent highly accurate registration of a specific bone or organ of interest, as long as the image data shows sufficient contrast. For CT data this might be realized using a suitable contrast agent. In return, the approximation could be improved using organ registration results of e.g. the kidneys.

In the future, the method will be validated on a larger dataset of mice with injected contrast agent. In addition, we plan to generalize the whole-body registration to other modalities as well. Thereby the focus will not only be on volumetric data (MRI or SPECT) but also on photographs from the subject surface (mono- or biplanar) for posture estimation, using skeleton based motion constraints.

5. ACKNOWLEDGEMENTS

The authors gratefully acknowledge Dr Paul Segars for providing us with the mouse atlas, the Biomedical Imaging Research Lab at the USC for the Digimouse atlas and Skyscan for providing the μCT scanner.

6. REFERENCES

[1] Segars et al. (2004), *Mol Im and Biol*, 6 (3): 149-159
[2] Dogdas et al. (2007), *Phys in Med and Biol*, 52(3): 577-587
[3] Alexandrakis et al. (2005), *Phys in Med and Biol*, 50(17): 4225-4241
[4] Chaudhari et al. (2007), *Proc. SPIE Med Im*, vol. 6510, 651024
[5] Li et al. (2007), *Proc. SPIE Med Im*, vol. 6512, 651202
[6] Kovacevic et al. (2003), *Proc. MICCAI*: 870-877
[7] Martin-Fernandez et al. (2005), *Proc. SPIE Med Im*, vol. 5747: 182-191
[8] Papademetris et al. (2005), *Proc. MICCAI*: 919-926
[9] Du Bois d'Aische et al. (2005), *Proc. IEEE Conf. on Im Proc.*, 1: 21-24
[10] Baiker et al. (2007), *Proc. IEEE ISBI 2007*: 728-731
[11] Bookstein (1989), *IEEE Trans PAMI*, 11(6): 567-585
[12] Besl et al. (1992), *IEEE Trans PAMI*, 14(2): 239-256
[13] Belongie et al. (2002), *IEEE Trans PAMI*, 24(24): 509-522
[14] Wang et al. (2003), *Comp Vis Im Unders*, 89(2-3): 252-271
[15] Wahba (1990), ISBN-13: 978-0898712445
[16] Sethian (1999), ISBN-13: 978-0521645577
[17] Bracco Altana Pharma GmbH, Konstanz, Germany
[18] ART Inc., Montreal, Canada